NASA Technical Memorandum 104600

# MODIS Airborne Simulator Visible and Near-Infrared Calibration - 1991 FIRE-Cirrus Field Experiment

## *Calibration Version - FIRE King 1.1*


**G. Thomas Arnold**
*Applied Research Corporation*
*Landover, Maryland*

**Michael D. King**
*Goddard Space Flight Center*
*Greenbelt, Maryland*

**Michael Fitzgerald**
**Patrick S. Grant**
*ATAC*
*Mountain View, California*




National Aeronautics and
Space Administration

**Goddard Space Flight Center**
Greenbelt, Maryland

**1994**

## Table of Contents

## I. Introduction

Calibration of the visible and near-infrared (near-IR) channels of the MODIS Airborne Simulator (MAS) is derived from observations of a calibrated light source. For the 1991 First ISSCP (International Satellite Cloud Climatology Project) Regional Experiment (the FIRE-Cirrus field deployment), the calibrated light source was the NASA Goddard 48-inch integrating hemisphere. Tests during the FIRE-Cirrus deployment were conducted to calibrate the hemisphere and then the MAS. This report summarizes the FIRE-Cirrus hemisphere calibration, and then describes how the MAS was calibrated from the hemisphere data. All MAS calibration measurements are presented and determination of the MAS calibration coefficients (raw counts to radiance conversion) is discussed. In addition comparisons to an independent MAS calibration by Ames personnel using their 30-inch integrating sphere is discussed.

## II. Hemisphere Calibration

During the FIRE-Cirrus deployment several calibrations of the Goddard 48-inch hemisphere were conducted. To calibrate the hemisphere, the hemisphere was operated at full intensity (all 12 lamps on) and the sphere output was measured at regular intervals over a broad wavelength range using an Optronic 746 Monochromater. For measurements in the visible wavelength region a silicon detector with a grating blazed at 0.75 μm was used, and for the longer near-IR wavelengths a germanium detector and a lead sulfide detector with gratings blazed at 1.6 μm and 2.5 μm respectively were used. These measurements were then calibrated from observations of a single standard lamp using the same monochromater. Table 1 summarizes the FIRE-Cirrus monochromater data (converted to radiance from the standard lamp observations). The Pre-FIRE-Cirrus column is the hemisphere calibration conducted just before shipping the hemisphere to Houston (this is a benchmark to note significant changes in the hemisphere data due to shipping). The FIRE-Cirrus Avg. column is the average radiance for each wavelength for all hemisphere calibrations conducted during the mission. In the last column are the standard deviation values for each FIRE-Cirrus Avg. radiance. The FIRE-Cirrus Avg. data are plotted vs. wavelength in Figure 1.

In addition to calibrating the hemisphere at full intensity (12 lamps), tests were also conducted to determine hemisphere radiance at less than 12 lamps. Starting with all 12 lamps on, radiance measurements at 0.05 μm intervals from 0.4 μm to 0.95 μm were recorded. Then lamps were turned off one at a time and the radiance recorded at each successively lower radiance. After all 12 levels had been recorded, the radiance values at lamp levels 1-11 were divided by the radiance at 12 lamps. This gives the relative change from full intensity for each lamp level. Since for each lamp level, the relative intensity values showed typically less than one percent variation over the different wavelengths, the relative intensities for each lamp level are considered independent of wavelength and have been averaged. The average relative intensity values for FIRE-Cirrus are shown in Table 2.

## III. MAS Calibration Procedure and Data

The MAS visible and near-IR channels are calibrated by observing different output intensities of the 48-inch hemisphere and correlating the observed MAS 'counts' values to the known hemisphere radiance values. For FIRE-Cirrus the calibration tests were conducted on three different days inside the ER-2 hangar in Houston. To conduct the calibration it was necessary to remove the instrument from the ER-2 wing pod and set it up on a stand directly in front of the 10 inch vertical opening in the flat side of the hemisphere. Then a front surface mirror was placed directly below the scan mirror, angled at 45° to both MAS nadir and the horizontal output beam of the hemisphere. Use of this mirror naturally degrades the observed radiance, and thus the spectral reflection of the mirror has been characterized. Table 3 lists the results of this characterization and its effect on each MAS channel.

Table 1. Hemisphere Radiance for 48-inch Hemisphere Before and During FIRE-Cirrus Mission, and the Standard Deviation of the FIRE-Cirrus Measurements.

| Wavelength (μm) | Pre-FIRE-Cirrus W/(m$^2$-μm-sr) | FIRE-Cirrus Avg W/(m$^2$-μm-sr) | Std. Dev. of FIRE Cirrus (Avg. in %) |
|---|---|---|---|
| 0.60 | 123.2 | 126.3 | 2.3 |
| 0.65 | 154.3 | 155.8 | 1.6 |
| 0.70 | 178.7 | 181.3 | 1.6 |
| 0.75 | 198.3 | 202.0 | 1.2 |
| 0.80 | 212.9 | 217.5 | 0.8 |
| 0.85 | 221.2 | 227.8 | 0.8 |
| 0.90 | 225.0 | 232.0 | 0.9 |
| 0.95 | 220.9 | 232.8 | 1.4 |
| 1.00 | 218.6 | 232.7 | 1.7 |
| 1.05 | 216.7 | 228.4 | 1.0 |
| 1.10 | 208.2 | 219.0 | 0.5 |
| 1.15 | 198.4 | 207.5 | 0.5 |
| 1.20 | 189.0 | 198.0 | 0.6 |
| 1.25 | 179.5 | 188.8 | 0.6 |
| 1.30 | 168.8 | 177.8 | 0.5 |
| 1.35 | 153.3 | 159.4 | 0.8 |
| 1.40 | 136.8 | 142.0 | 1.4 |
| 1.45 | 127.1 | 132.9 | 1.6 |
| 1.50 | 122.8 | 126.8 | 1.3 |
| 1.55 | 115.2 | 120.6 | 2.7 |
| 1.60 | 110.4 | 104.4 | 4.1 |
| 1.65 | 102.8 | 104.4 | 3.5 |
| 1.70 | 93.8 | 95.7 | 3.2 |
| 1.75 | 84.2 | 86.8 | 4.5 |
| 1.80 | 76.8 | 79.8 | 3.2 |
| 1.85 | 67.0 | 70.9 | 4.0 |
| 1.90 | 53.7 | 54.2 | 3.7 |
| 1.95 | 51.5 | 51.2 | 7.1 |
| 2.00 | 48.3 | 52.3 | 3.2 |
| 2.05 | 47.3 | 49.8 | 2.2 |
| 2.10 | 43.0 | 44.7 | 1.3 |
| 2.15 | 39.1 | 42.4 | 6.7 |

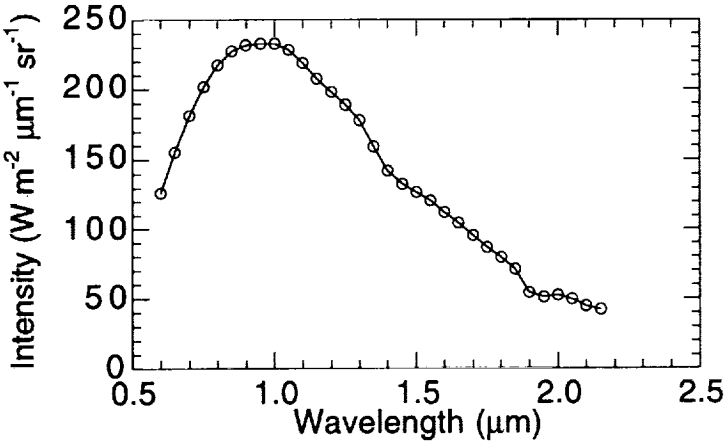


Figure 1. Plot of average hemisphere intensity (FIRE-Cirrus Avg column in Table 1) vs. wavelength.

Table 2. Average Relative Intensity for Each Hemisphere Lamp for all Measurements Between 0.4 and 0.95 μm

| No. of Lamps Turned On | Relative Intensity |
|---|---|
| 12 | 1.000 |
| 11 | 0.912 |
| 10 | 0.834 |
| 9 | 0.750 |
| 8 | 0.659 |
| 7 | 0.579 |
| 6 | 0.498 |
| 5 | 0.413 |
| 4 | 0.325 |
| 3 | 0.250 |
| 2 | 0.163 |
| 1 | 0.084 |

Table 3. Characterization of the Front Surface Mirror Used in MAS Calibration and Interpolation of Reflectance Values to MAS Wavelengths

| Wavelength (μm) | Average Reflectance (%) | MAS wavelength (μm) | Reflectance (%) |
|---|---|---|---|
| 0.60 | 89.68 | | |
| 0.65 | 86.24 | 0.681 | 84.51 |
| 0.70 | 83.45 | | |
| 0.75 | 79.48 | | |
| 0.80 | 75.38 | | |
| 0.85 | 72.98 | | |
| 0.90 | 78.81 | | |
| 0.95 | 83.57 | | |
| 1.00 | 87.85 | | |
| 1.05 | 90.35 | | |
| 1.10 | 91.37 | | |
| 1.15 | 92.57 | | |
| 1.20 | 93.49 | | |
| 1.25 | 94.19 | | |
| 1.30 | 94.64 | | |
| 1.35 | 94.98 | | |
| 1.40 | 95.51 | | |
| 1.45 | 95.78 | | |
| 1.50 | 96.39 | | |
| 1.55 | 95.92 | | |
| 1.60 | 96.75 | 1.6170 | 97.07 |
| 1.65 | 97.70 | | |
| 1.70 | 96.59 | | |
| 1.75 | 98.89 | | |
| 1.80 | 98.24 | | |
| 1.85 | 99.01 | | |
| 1.90 | 97.69 | 1.9330 | 97.06 |
| 1.95 | 96.73 | | |
| 2.00 | 99.37 | | |
| 2.05 | 96.20 | 2.0880 | 96.20 |
| 2.10 | 96.20 | 2.1390 | 97.20 |
| 2.15 | 97.48 | | |

With the MAS carefully aligned with the hemisphere radiance, starting at full intensity (12 lamps), then turning off lamps one at a time, observations of each hemisphere radiance level were recorded. Table 4 (a-e) summarizes by channel all the MAS calibration measurements taken during FIRE. Note that channels 2-6 are all recorded at 8 bits and thus all counts values in Table 4 are between 0 and 255.

Since MAS counts values are by design linearly proportional to radiance, a radiance per count factor for each channel can be determined by a simple linear regression of the MAS counts for each channel and the associated hemisphere radiance values. Thus appropriate hemisphere radiance values must be determined for each of MAS channels 2-6. One method is to determine the hemisphere radiance at the wavelength of the peak power point of the spectral response curve for each channel's bandpass filter function. Then interpolate from the values in Table 1 the appropriate hemisphere radiance. A second method is to interpolate the hemisphere data for the wavlength region of the bandpass filter for each channel and then integrate over the entire bandpass filter. Generally the second method is preferable, however for the FIRE-Cirrus data, the first method has been chosen. Using the interpolated radiance at the filter's peak power point is considered adequate due to the relatively narrow MAS bandwidths (equal to or only slightly greater than the 0.05μm sampling interval for the hemisphere data), and as will be shown in the final section of this report, the differences in the two methods of radiance determination are less than 2% and thus are smaller than the standard deviation values of the hemisphere calibration. Furthermore measured spectral response curves are unavailable for channels 4 and 5 and thus integration over the bandpass filter function is not possible for these channels.

The result of each linear regression of MAS counts and their associated radiance values is a radiance per count factor (slope) and a radiance offset (intercept). The radiance/count and radiance offset values for the 7 tests are given in Tables 5 (a-e). Generally the results show good agreement in tests 3, 4, 5, 6, and 7. However (except for channel 2) the radiance/count values for tests 1 and 2 are consistently higher than those of the other tests, particularly for channels 4, 5 and 6. Environmental conditions for these two tests however were much different than for the others. The humidity had increased significantly from the previous day. The dew point had increased to about 70°F and the relative humidity was at least 70%. Relative humidity on the other days were typically in the 30-50% range. Calibration of the hemisphere on this day showed no significant change in the hemisphere radiance as compared to the other less humid days. Thus this suggests somehow the high humidity was adversely affecting the MAS directly.

As an explanation for the discrepancies in tests 1 and 2, recent experience with the MAS calibration has shown that 20-30 minutes is needed for the instrument to return completely to nominal counts after filing the dewars with liquid $N_2$ (LN2) in moderately humid conditions. The effect is observed to be related to the humidity level. It is presumed that the LN2 vapors cool the dewar window and focusing lenses to below the dew point. (Dew is often observed after filling). Thus unintentional fogging of the optics occurs initially but then begins to dry out as the ambient temperature rises due to the heat generated by both the instrument and the integrating hemisphere. This principle is supported by increased (and somewhat more realistic) count values in test 2 (test 2 was conducted less than 30 minutes after test 1). Therefore sufficient evidence exists to justify not using any of the high humidity data in determining the final calibration coefficients. Furthermore note that specific plans to incorporate better temperature stability, LN2 venting, and humidity reduction will be instituted for all calibrations beginning in the spring of 1994 to alleviate such future problems. Also relative calibrations (soon to be absolute calibrations) are now taken prior to every flight. This allows for a statistical approach to be taken and bad data to be investigated and thrown out if necessary.

Table 4 (a-e). Summary of All MAS Hemisphere Observations for FIRE-Cirrus

(a)
Channel 2 - 0.681 μm

| No. of lamps | 11/16/91 Test 1 | 11/16/91 Test 2 | 11/20/91 Test 3 | 11/20/91 Test 4 | 11/20/91 Test 5 | 11/23/91 Test 6 | 11/23/91 Test 7 |
|---|---|---|---|---|---|---|---|
| 12 | 204 | data | 102 | 206 | 102 | 204 | 101 |
| 11 | 185 | not | 94 | 188 | 93 | 187 | 92 |
| 10 | 172 | avail- | 86 | 173 | 85 | 171 | 85 |
| 9 | 155 | able | 78 | 156 | 77 | 155 | 77 |
| 8 | 135 | | 68 | 139 | 68 | 137 | 68 |
| 7 | 120 | | 60 | 122 | 60 | 121 | 60 |
| 6 | 105 | | 53 | 107 | 53 | 107 | 53 |
| 5 | 89 | | 44 | 89 | 45 | 91 | 45 |
| 4 | 72 | | 36 | 72 | 37 | 75 | 37 |
| 3 | 57 | | 28 | 58 | 30 | 59 | 29 |
| 2 | 42 | | 21 | 42 | 21 | 43 | 21 |
| 1 | 27 | | 13 | 26 | 14 | 27 | 14 |
| 0 | 10 | | 5 | 10 | 4 | 11 | 5 |
| gain | 2 | | 1 | 2 | 1 | 2 | 1 |

(b)
Channel 3 - 1.617 μm

| No. of lamps | 11/16/91 Test 1 | 11/16/91 Test 2 | 11/20/91 Test 3 | 11/20/91 Test 4 | 11/20/91 Test 5 | 11/23/91 Test 6 | 11/23/91 Test 7 |
|---|---|---|---|---|---|---|---|
| 12 | 224 | | | | | | |
| 11 | 206 | | | | | 235 | |
| 10 | 189 | | | 220 | | 216 | |
| 9 | 171 | | | 198 | | 194 | |
| 8 | 152 | | | 175 | | 171 | |
| 7 | 133 | | | 153 | | 151 | |
| 6 | 116 | | | 132 | | 131 | |
| 5 | 97 | 219 | 221 | 110 | 221 | 110 | 222 |
| 4 | 78 | 176 | 177 | 80 | 179 | 89 | 179 |
| 3 | 60 | 134 | 135 | 67 | 136 | 68 | 137 |
| 2 | 42 | 94 | 94 | 47 | 95 | 47 | 95 |
| 1 | 24 | 52 | 52 | 26 | 52 | 26 | 52 |
| 0 | 4 | 9 | 9 | 4 | 9 | 4 | 9 |
| gain | 1 | 2 | 2 | 1 | 2 | 1 | 2 |

(c)
Channel 4 - 1.933 μm

| No. of lamps | 11/16/91 Test 1 | 11/16/91 Test 2 | 11/20/91 Test 3 | 11/20/91 Test 4 | 11/20/91 Test 5 | 11/23/91 Test 6 | 11/23/91 Test 7 |
|---|---|---|---|---|---|---|---|
| 12 | 199 | | | | | | |
| 11 | 184 | | | | | | |
| 10 | 171 | | | | | | |
| 9 | 157 | | | | | | |
| 8 | 141 | | | | | | |
| 7 | 125 | | | | | | |
| 6 | 110 | | | | | | |
| 5 | 93 | | | 226 | | 229 | |
| 4 | 77 | | | 181 | | 185 | |
| 3 | 60 | | | 138 | | 140 | |
| 2 | 43 | | | 95 | | 97 | |
| 1 | 26 | 159 | 212 | 53 | 212 | 53 | 214 |
| 0 | 8 | 33 | 34 | 8 | 33 | 8 | 33 |
| gain | 2 | 8 | 8 | 2 | 8 | 2 | 8 |

(d)
Channel 5- 2.088 μm

| No. of lamps | 11/16/91 Test 1 | 11/16/91 Test 2 | 11/20/91 Test 3 | 11/20/91 Test 4 | 11/20/91 Test 5 | 11/23/91 Test 6 | 11/23/91 Test 7 |
|---|---|---|---|---|---|---|---|
| 12 | 215 | | | | | | |
| 11 | 200 | | | | | | |
| 10 | 186 | | | | | | |
| 9 | 171 | | | | | | |
| 8 | 155 | | | | | | |
| 7 | 139 | | | | | | |
| 6 | 124 | | | | | | |
| 5 | 107 | | | 227 | | 225 | |
| 4 | 90 | | | 184 | | 185 | |
| 3 | 73 | 223 | | 143 | | 143 | |
| 2 | 56 | 166 | 206 | 103 | 206 | 103 | 207 |
| 1 | 39 | 106 | 126 | 63 | 124 | 63 | 125 |
| 0 | 21 | 42 | 42 | 21 | 42 | 21 | 42 |
| gain | 4 | 8 | 8 | 4 | 8 | 4 | 8 |

(e)
Channel 6 - 2.139 μm

| No. of lamps | 11/16/91 Test 1 | 11/16/91 Test 2 | 11/20/91 Test 3 | 11/20/91 Test 4 | 11/20/91 Test 5 | 11/23/91 Test 6 | 11/23/91 Test 7 |
|---|---|---|---|---|---|---|---|
| 12 | 215 | | | | | | |
| 11 | 199 | | | | | | |
| 10 | 185 | | | | | | |
| 9 | 171 | | | | | | |
| 8 | 155 | | | | | | |
| 7 | 138 | | | | | | |
| 6 | 122 | | | 225 | | 222 | |
| 5 | 105 | | | 190 | | 188 | |
| 4 | 87 | 252 | | 154 | | 154 | |
| 3 | 70 | 199 | 238 | 119 | 238 | 119 | 239 |
| 2 | 53 | 146 | 171 | 86 | 171 | 86 | 172 |
| 1 | 35 | 91 | 103 | 52 | 102 | 51 | 102 |
| 0 | 16 | 32 | 33 | 16 | 33 | 16 | 33 |
| gain | 4 | 8 | 8 | 4 | 8 | 4 | 8 |

Table 5. MAS Calibration Coefficients for Each Visible and Near-IR Channel and the Dates They Were Determined

(a)
Channel 2 - 0.681 μm

| Test No. | Date | Correlation Coefficient | Rad/Count* (Slope) | Radiance offset† (Intercept) |
|---|---|---|---|---|
| 1 | 11/16/91 | 0.99985 | 1.503E+00 | -7.200E+00 |
| 2 | 11/16/91 | 0.99985 | 1.502E+00 | -7.198E+00 |
| 3 | 11/20/91 | 0.99983 | 1.488E+00 | -6.592E+00 |
| 4 | 11/20/91 | 0.99995 | 1.479E+00 | -6.843E+00 |
| 5 | 11/20/91 | 0.99985 | 1.528E+00 | -8.380E+00 |
| 6 | 11/23/91 | 0.99991 | 1.516E+00 | -8.424E+00 |
| 7 | 11/23/91 | 0.99986 | 1.523E+00 | -7.988E+00 |

(b)
Channel 3 - 1.617 μm

| Test No. | Date | Correlation Coefficient | Rad/Count* (Slope) | Radiance offset† (Intercept) |
|---|---|---|---|---|
| 1 | 11/16/91 | 0.99992 | 4.840E-01 | -2.716E+00 |
| 2 | 11/16/91 | 0.99979 | 4.174E-01 | -1.833E+00 |
| 3 | 11/20/91 | 0.99985 | 4.135E-01 | -1.748E+00 |
| 4 | 11/20/91 | 0.99941 | 4.097E-01 | -1.039E+00 |
| 5 | 11/20/91 | 0.99975 | 4.109E-01 | -1.706E+00 |
| 6 | 11/23/91 | 0.99965 | 4.278E-01 | -2.506E+00 |
| 7 | 11/23/91 | 0.99979 | 4.107E-01 | -1.725E+00 |

Table 5 (con't). MAS Calibration Coefficients for Each Visible and Near-IR Channel and the Dates They Were Determined

(c)
Channel 4 - 1.933 μm

| Test No. | Date | Correlation Coefficient | Rad/Count* (Slope) | Radiance offset† (Intercept) |
|---|---|---|---|---|
| 1 | 11/16/91 | 0.99913 | 5.392E-01 | -3.221E+00 |
| 2 | 11/16/91 | 0.99973 | 5.297E-01 | -2.171E+00 |
| 3 | 11/20/91 | 1.00000 | 1.928E-01 | -7.712E-01 |
| 4 | 11/20/91 | 0.99989 | 1.957E-01 | -8.048E-01 |
| 5 | 11/20/91 | 1.00000 | 1.928E-01 | -7.712E-01 |
| 6 | 11/23/91 | 0.99974 | 1.925E-01 | -7.625E-01 |
| 7 | 11/23/91 | 1.00000 | 1.950E-01 | -7.798E-01 |

(d)
Channel 5 - 2.088 μm

| Test No. | Date | Correlation Coefficient | Rad/Count* (Slope) | Radiance offset† (Intercept) |
|---|---|---|---|---|
| 1 | 11/16/91 | 0.99927 | 1.007E+00 | -6.091E+00 |
| 2 | 11/16/91 | 0.99910 | 5.339E-01 | -2.827E+00 |
| 3 | 11/20/91 | 1.00000 | 3.856E-01 | -1.935E+00 |
| 4 | 11/20/91 | 0.99985 | 3.926E-01 | -1.999E+00 |
| 5 | 11/20/91 | 0.99984 | 3.856E-01 | -1.887E+00 |
| 6 | 11/23/91 | 0.99977 | 3.950E-01 | -1.993E+00 |
| 7 | 11/23/91 | 0.99978 | 3.833E-01 | -1.867E+00 |

(e)
Channel 6- 2.139 μm

| Test No. | Date | Correlation Coefficient | Rad/Count* (Slope) | Radiance offset† (Intercept) |
|---|---|---|---|---|
| 1 | 11/16/91 | 0.99911 | 8.826E-01 | -4.466E+00 |
| 2 | 11/16/91 | 0.99969 | 5.232E-01 | -2.195E+00 |
| 3 | 11/20/91 | 0.99970 | 4.247E-01 | -1.760E+00 |
| 4 | 11/20/91 | 0.99976 | 4.245E-01 | -1.735E+00 |
| 5 | 11/20/91 | 0.99966 | 4.235E-01 | -1.713E+00 |
| 6 | 11/23/91 | 0.99980 | 4.236E-01 | -1.770E+00 |
| 7 | 11/23/91 | 0.99960 | 4.210E-01 | -1.697E+00 |

* Radiance/count values have units of W $m^{-2}$ $\mu m^{-1}$ $sr^{-1}$ $cnt^{-1}$
† Radiance offset values have units of W $m^{-2}$ $\mu m^{-1}$ $sr^{-1}$.

To determine the actual calibration coefficients to apply to the FIRE-Cirrus data, an average of all the tests (except for the high humidity calibration data of tests 1 and 2) has been calculated. Note however the values were first averaged for each day and then the daily values were averaged. The results are presented in Table 6 (a,b). Two tables are necessary to present the coefficients due to a calibration change in channel 2 that occurred November 15. Analysis of flight data from 14 November showed that channel 2 data were 'clipping' at 122 counts (gain setting of 0.5). This clipping was due to an electronic saturation that forced all data that would have been greater than 122 to be recorded at 122 counts. To compensate for the clipping problem a resistor inside the MAS was changed. According to the factory specifications for the type of resistor installed, the resulting gain change is estimated to be (within about one percent) a factor of 2. Since all the calibration data in Table 5 were taken after this resistor change, the channel 2 radiance/count value in Table 6 (a) is a factor of two smaller

than in Table 6 (b). All data for channels 3, 4, 5, and 6 Table 6 (a,b) are the same.

Also note in Table 6 that the intercept values have not been included. These data are not necessary for final calibration because in-flight the MAS references the cold internal blackbody as a visible zero target. The number of counts each of the visible and near-IR channels 'sees' when observing the blackbody is considered zero radiance. These counts at zero radiance are the system offset and are independent of the magnitude of the radiance/count values. Thus to properly calibrate an in-flight counts value this offset must be first subtracted from the earth view count. The offset corrected earth view count is then multiplied by the radiance/count factor in Table 6 below. (Note these offset values are always recorded by the MAS data system at a gain of 1.0 and must therefore by multiplied by the gain setting before being subtracted from the earth view counts.)

Table 6 Final Radiance/Count (Slope) Values for FIRE-Cirrus, Valid for Gain Setting of 1.0

(a)

| Counts to radiance conversion for data collected October 31 - November 14, 1991 | | |
|---|---|---|
| Channel | Wavelength (μm) | Radiance/Count W $m^{-2}$ $\mu m^{-1}$ $sr^{-1}$ $cnt^{-1}$ |
| 2 | 0.681 | 7.492E-01 |
| 3 | 1.617 | 4.114E-01 |
| 4 | 1.933 | 1.938E-01 |
| 5 | 2.088 | 3.879E-01 |
| 6 | 2.139 | 4.242E-01 |

(b)

| Counts to radiance conversion for data collected November 15-December 7, 1991 | | |
|---|---|---|
| Channel | Wavelength (μm) | Radiance/Count W $m^{-2}$ $\mu m^{-1}$ $sr^{-1}$ $cnt^{-1}$ |
| 2 | 0.681 | 1.498E+00 |
| 3 | 1.617 | 4.114E-01 |
| 4 | 1.933 | 1.938E-01 |
| 5 | 2.088 | 3.879E-01 |
| 6 | 2.139 | 4.242E-01 |

Note: Divide radiance/count values in above tables by the in-flight gain setting to derive the actual value to apply to the raw data counts.

## IV. Temperature Sensitivity of MAS Calibration

During the FIRE-Cirrus deployment, the MAS typically cooled in-flight to near -30°C (significantly colder than the +25°C laboratory calibration environment). However due to a design problem in the port 2 dewar (housing the near-IR detectors), the calibration of the near-IR channels change as the instrument cools in-flight. The problem with this early dewar design was that the detectors were mounted by a stem to the top of the dewar, causing the detectors to follow the movement of the outer case of the dewar. Thus the detectors tend to shift out of the beam as the dewar outer case is cooled (by the cold ambient air temperatures). Due to very limited time in preparing the MAS for its maiden deployment, there was no time to address this problem before the FIRE-Cirrus mission. Note however subsequent to the mission, heater jackets were added to the dewars to partially heat the dewar, reducing the movement to about 1/4 of what it was. New dewars scheduled for installation in the spring

of 1994 will eliminate the problem altogether.

To characterize the sensitivity of the calibration of the port 2 near-IR channels to instrument temperature, calibration tests were conducted inside a cold chamber at Ames following the FIRE-Cirrus mission in February 1992. In the cold chamber, a light box was placed directly below the MAS. Starting at room temperature (and atmospheric pressure) the light box radiance was measured. Then the chamber was cooled. At temperatures of 0, -23 and -35°C, the cooling was temporarily stopped, the chamber allowed to stabilize, and the light box measurements recorded. The results are summarized in Table 7 and suggest a calibration change with instrument temperature for the MAS near-IR channels 3-6 ranging from 33 to about 42%. Note MAS channel 2 (port 1 - 0.68 μm) data showed no appreciable change with temperature in the chamber, and thus has not been included in the table. Also because of lack of change in the channel 2 data, the light box radiance is assumed constant for all wavelengths and temperatures investigated.

Table 7. Summary of Post-FIRE-Cirrus Cold Chamber Data Tests, Temperatures are in °C and Channel Values and Offsets are in Raw Counts

| Temperature | Channel 3 | Channel 4 | Channel 5 | Channel 6 |
|---|---|---|---|---|
| 25 | 238 | 151 | 142 | 233 |
| 0 | 220 | 140 | 123 | 199 |
| -23 | 198 | 119 | 106 | 171 |
| -35 | 165 | 100 | 89 | 142 |
| offsets | 20 | 8 | 10 | 16 |
| gain setting | 4 | 2 | 2 | 4 |
| % change | 33.5 | 35.7 | 40.2 | 41.9 |

Note: The gain settings apply to all count values in the table. Offset values are subtracted from each channel value before computing % change from +25 to -35°C.

Due to the temperature sensitivity of MAS channels 3-6 indicated in Table 7, the laboratory calibration values in Table 6 are not directly applicable to in-flight earth view counts data. To enable such usage of the laboratory coefficients, an adjustment to the in-flight earth view counts is necessary to correct for this temperature sensitivity. However before quantitatively defining this adjustment, it is necessary to first define the instrument temperature (upon which the adjustment is dependent). Determination of instrument temperature ($T_{mas}$) is complicated by different cooling rates of different instrument components due to their degree of exposure to the cold environment, mass, and position relative to heated components of the instrument. To monitor the temperature a Rustrak recording system with one thermistor was used. The thermistor was placed near the optics housing and is considered a much better measurement of 'true' instrument temperature than the ambient blackbody thermistor. Unfortunately due again to the strict time constraints of getting the MAS ready for its maiden deployment, the magnitude of the temperature sensitivity problem at the time of the deployment was not fully realized. Likewise only a limited amount of Rustrak data were recorded during the FIRE mission, and as will be discussed more below, placement of the thermistor could have been more optimal. Figure 2 below summarizes the Rustrak temperature data and also ambient blackbody temperature data (shown for comparison) for four consecutive flights during the FIRE-Cirrus deployment. Analysis of these data (and similar analysis of Rustrak temperature data from the subsequent ASTEX and TOGA/COARE missions) shows that $T_{mas}$ can be adequately described by an average of the Rustrak curves. Figure 3 shows that the difference for each of the 4 curves from the average curve is generally less than 3 degrees (resulting in less than 4% error in the final calibration). The lower curve in Figure 4 shows the average curve for the FIRE-Cirrus data.

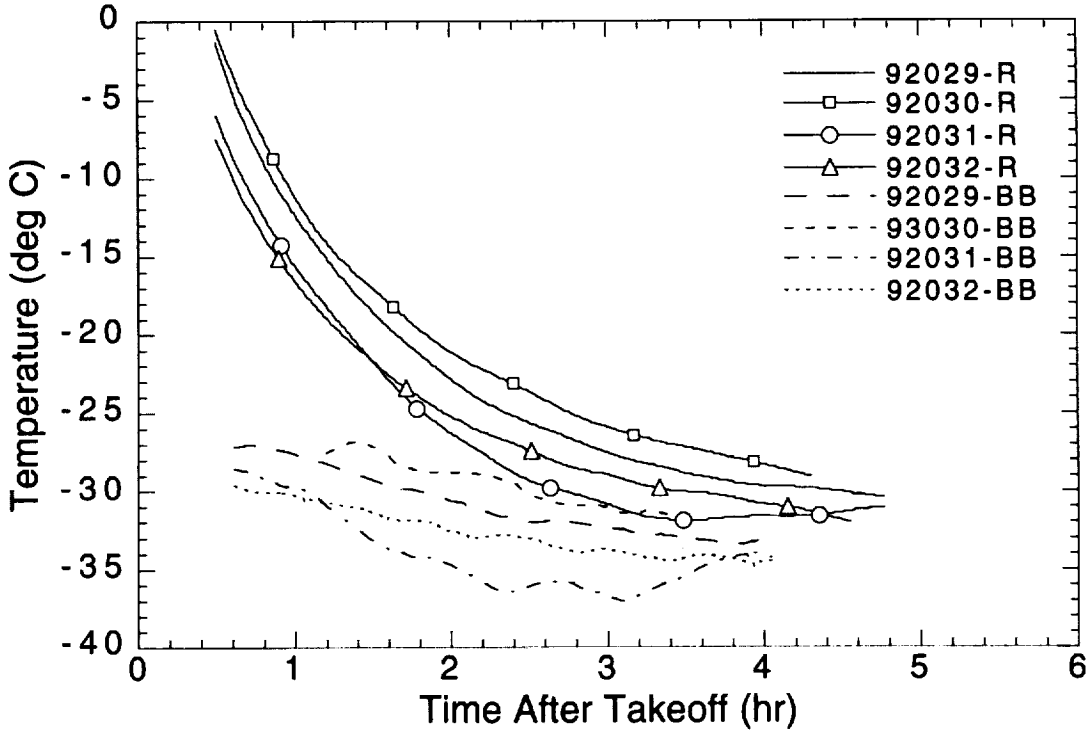


Figure 2. Rustrak (R) and ambient blackbody temperature (BB) data for FIRE-Cirrus. Flights are listed by sortie number. Note the large temperature difference between the blackbody and Rustrak temperatures early in each flight, indicating how much more quickly the blackbody temperature responds to the rapid drop in environmental temperature as the ER-2 quickly climbs to cruise altitude.

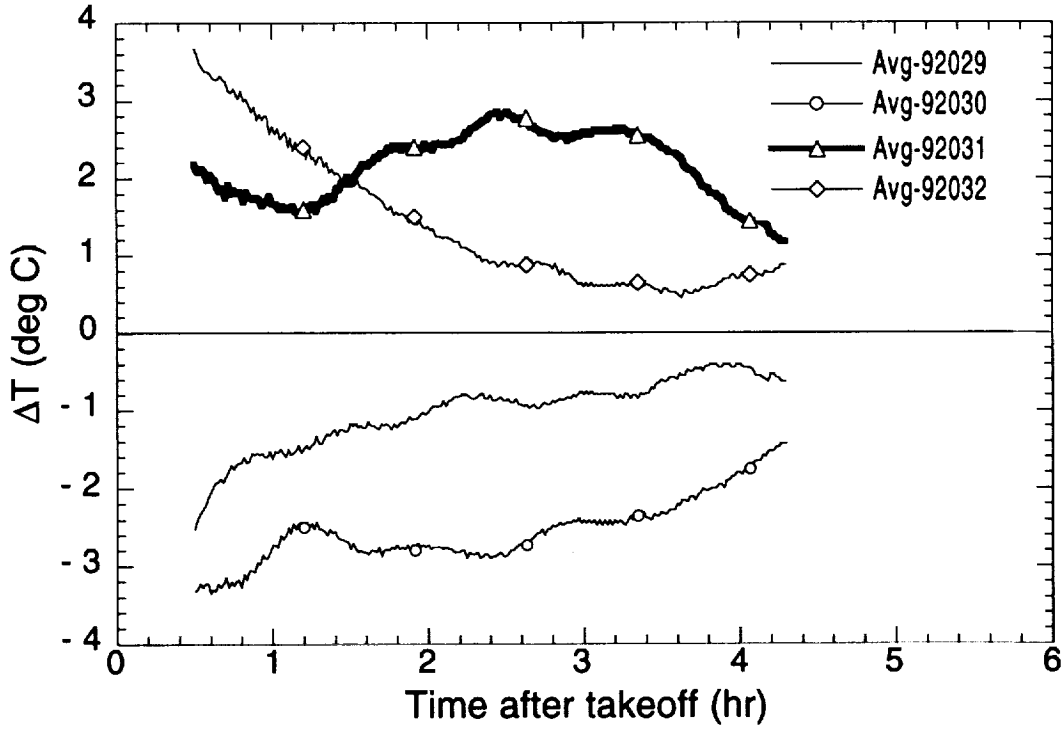


Figure 3. Difference between the average Rustrak temperature and the actual temperature measured for each flight Rustrak data were recorded, as a function of time after takeoff.

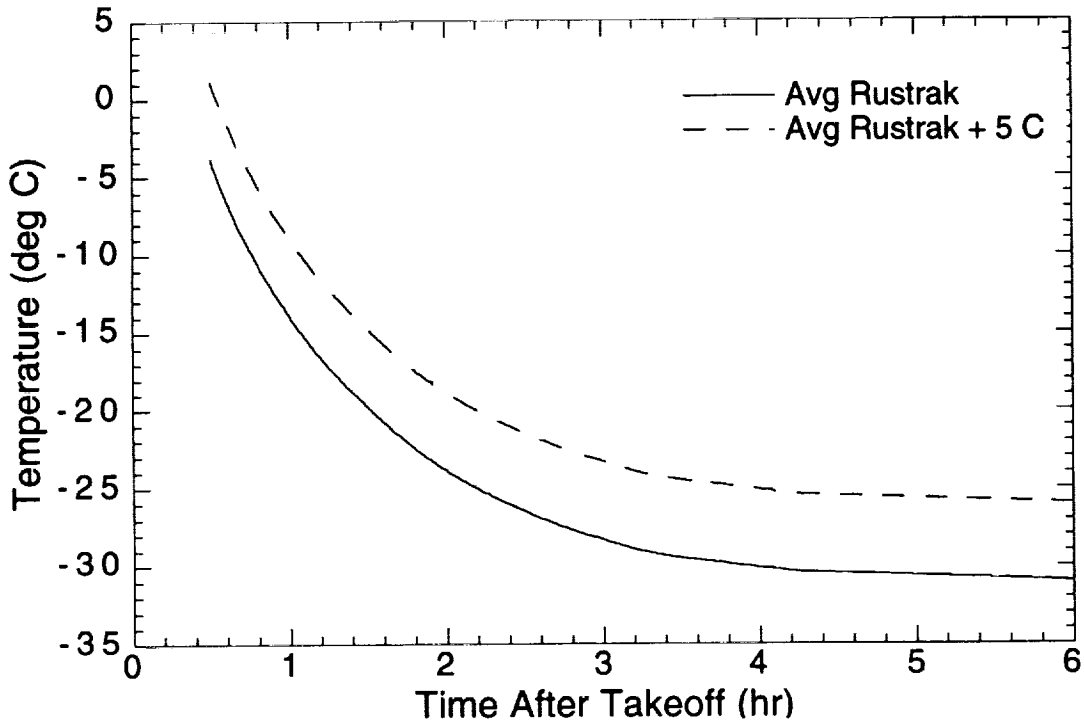


Figure 4. Average curve for FIRE-Cirrus Rustrak temperature data, extrapolated to 6 hours after takeoff. Dashed line curve is the 'corrected' Rustrak temperature curve (used to derive the curve fit). This curve is simply the lower curve + 5°C.

Figure 4 also shows a second curve. This curve is simply the average Rustrak curve plus 5°C added at each point. Use of this curve to represent $T_{mas}$, rather than just the average curve, is suggested primarily due to the placement of the Rustrak thermistor. The thermistor for the FIRE-Cirrus flights was taped on the electronics near, but not on, the optics housing. In subsequent missions, the thermistor has been glued directly to the optics housing. Placement of the thermistor on the electronics results in the thermistor being slightly more sensitive to the cold environmental air temperature and than if it were placed on the more slowly cooling optics housing. This is quantitatively depicted in Figure 5, showing a comparison of the difference between the average Rustrak temperature and the average ambient blackbody temperature as a function of time after takeoff, for three MAS deployments. Following takeoff, the thermistor on the surface of the ambient blackbody, relative to the Rustrak thermistor, responds quite quickly to the rapidly decreasing environmental temperature. Hence the large temperature difference early in the flight, then decreasing as the flight progresses and the environmental temperature stabilizes. Note the much smaller temperature difference for the FIRE-Cirrus data (even though the actual environmental temperatures were appreciably warmer in ASTEX). Thus as an estimate to compensate for the placement of the FIRE-Cirrus Rustrak thermistor, 5°C has been added to the data. Therefore to quantitatively define $T_{mas}$ for all FIRE-Cirrus flights, a curve-fit has been applied to the average + 5°C curve in Figure 4. Tests using a polynomial least squares curve fit technique, show that for this case the best-fit is provided by a polynomial expression of at least the fourth order. The fourth order polynomial is given in equation 1 below:

$$T_{mas} = M_0 + M_1*T_{dh} + M_2*(T_{dh})^2 + M_3*(T_{dh})^3 + M_4*(T_{dh})^4, \quad \text{where,} \qquad (1)$$

$T_{dh}$ is the time (in decimal hours) from takeoff
$M_0$ = 1.2631E+01
$M_1$ =-2.8631E+01
$M_2$ = 8.5601E+00
$M_3$ =-1.1984E+00
$M_4$ = 6.4870E-02

Note that this expression is valid only from 0.5 to about 6 hours after takeoff. Typically it takes about 30 minutes after takeoff for the ER-2 to get to cruise altitude. The temperature in this first 30 minutes is most strongly influenced by the takeoff temperature which can be quite variable. Once the plane reaches altitude the temperature is much less variable day to day. The 6 hour cutoff is used since no MAS FIRE-Cirrus flights exceeded 6 hours.

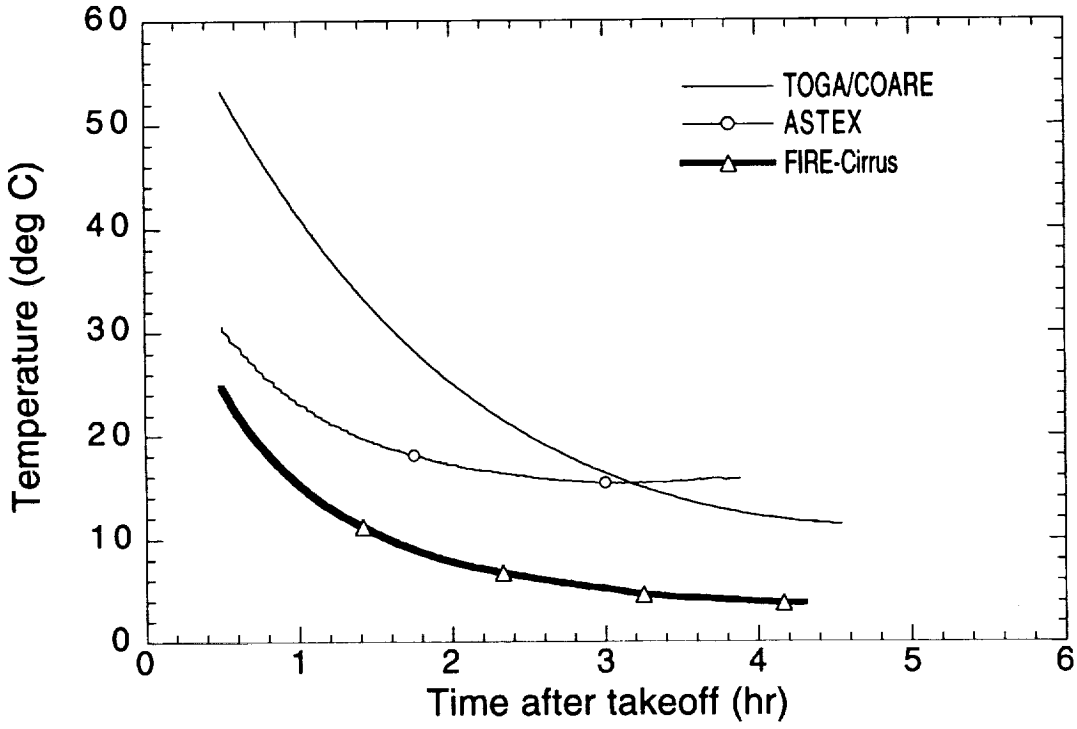


Figure 5. Average Rustrak temperature minus the average ambient blackbody temperature, as a function of time after takeoff, for three MAS deployments.

Using $T_{mas}$ as described above, expressions to characterize the change in calibration with temperature for each temperature sensitive channel are derived. These expressions 'adjust' the earth-view counts values to what that value would be if the measurement were taken at laboratory (+25°C) conditions. This adjustment then makes the calibration coefficients described previously (in Table 6) applicable to in-flight data. To derive these equations, the data in Table 7 is used. Table 7 shows the MAS counts change with change in temperature for channels 3-6. This counts change with temperature however is valid only for the particular radiance of the light box and the MAS gain settings for each channel during the test. To apply these results more generally, it is necessary to compute the ratio of the change in the MAS counts from the +25°C measurement. Table 8 summarizes the results of this calculation for each channel. Each data entry in the table was calculated by first subtracting the appropriate offset values from each counts value in Table 7, then using only the resulting count values, for each channel the counts value at each temperature was subtracted from the counts at +25°C. This difference was then divided by the counts at +25°C, resulting in a ratio, for each temperature, of the change in counts from +25°C to the value at +25°C. At 25°C the ratio is of course zero, but indicating the temperature sensitivity, the ratio increases as the MAS cools. The ratio values are graphically depicted by the data points shown in Figures 6-9. By fitting an exponential curve to these data points, a relationship describing the ratio of the change in MAS measurement as a function of temperature is derived for each channel. Following are the equations describing the curve fits:

Channel 3:

$$\Delta mas_1 = m_1 + m_2 * \exp(-m_3 * T_{mas}), \quad \text{where,} \tag{2}$$

$\Delta mas_1$ = the ratio of the change in MAS counts from +25°C to the value at instrument temperature $T_{mas}$ divided by the counts at +25°C (with offsets subtracted from all counts values)

$m_1$ =-0.02637
$m_2$ = 0.09183
$m_3$ = 0.03872

Channel 4:

$$\Delta mas_2 = m_1 + m_2 * \exp(-m_3 * T_{mas}), \quad \text{where} \tag{3}$$

$m_1$ =-0.06322
$m_2$ = 0.13954
$m_3$ = 0.03148

Channel 5:

$$\Delta mas_3 = m_1 + m_2 * \exp(-m_3 * T_{mas}), \quad \text{where} \tag{4}$$

$m_1$ =-0.31486
$m_2$ = 0.44537
$m_3$ = 0.01329

Table 8. Ratio of the Change from Laboratory Conditions (+25°C) of MAS Counts for Each Temperature Measurement Recorded During the Post-FIRE-Cirrus Cold Chamber Data Test.

| Temperature | Channel 3 | Channel 4 | Channel 5 | Channel 6 |
|---|---|---|---|---|
| 25 | 0 | 0 | 0 | 0 |
| 0 | 0.083 | 0.077 | 0.144 | 0.157 |
| -23 | 0.183 | 0.224 | 0.273 | 0.286 |
| -35 | 0.335 | 0.357 | 0.402 | 0.419 |

Note: Offset values were first subtracted from each counts value in Table 7, then using these modified counts values, the difference in counts of each temperature from the +25°C value was calculated then divided by the counts value at 25°C to get the ratio values in the above table.

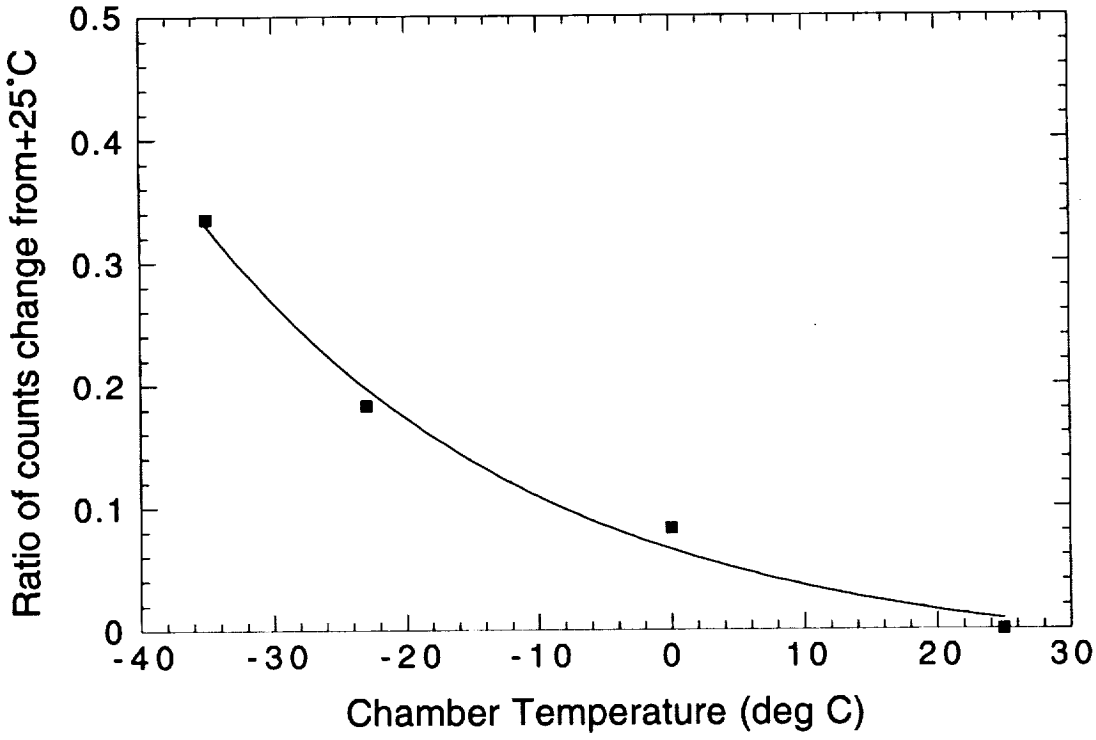


Figure 6. Ratio of the change from laboratory conditions (+25°C) of MAS channel 3 counts to decreasing instrument temperature. Solid line is an exponential best fit curve.

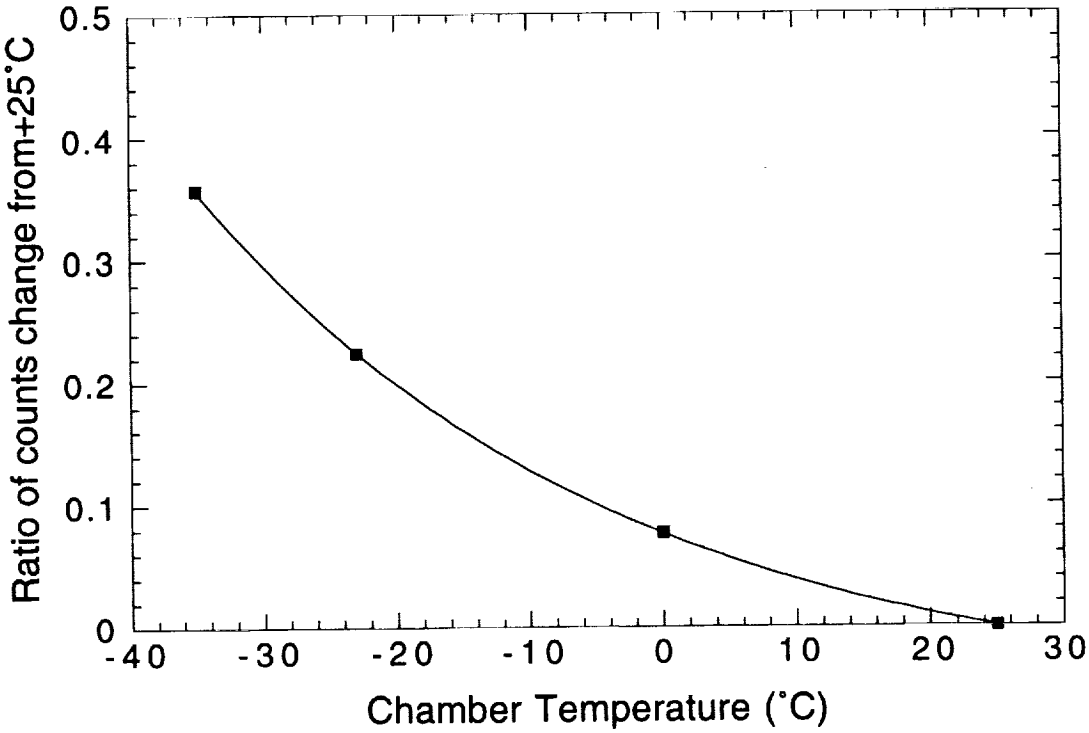


Figure 7. Ratio of the change from laboratory conditions (+25°C) of MAS channel 4 counts to decreasing instrument temperature. Solid line is an exponential best fit curve.

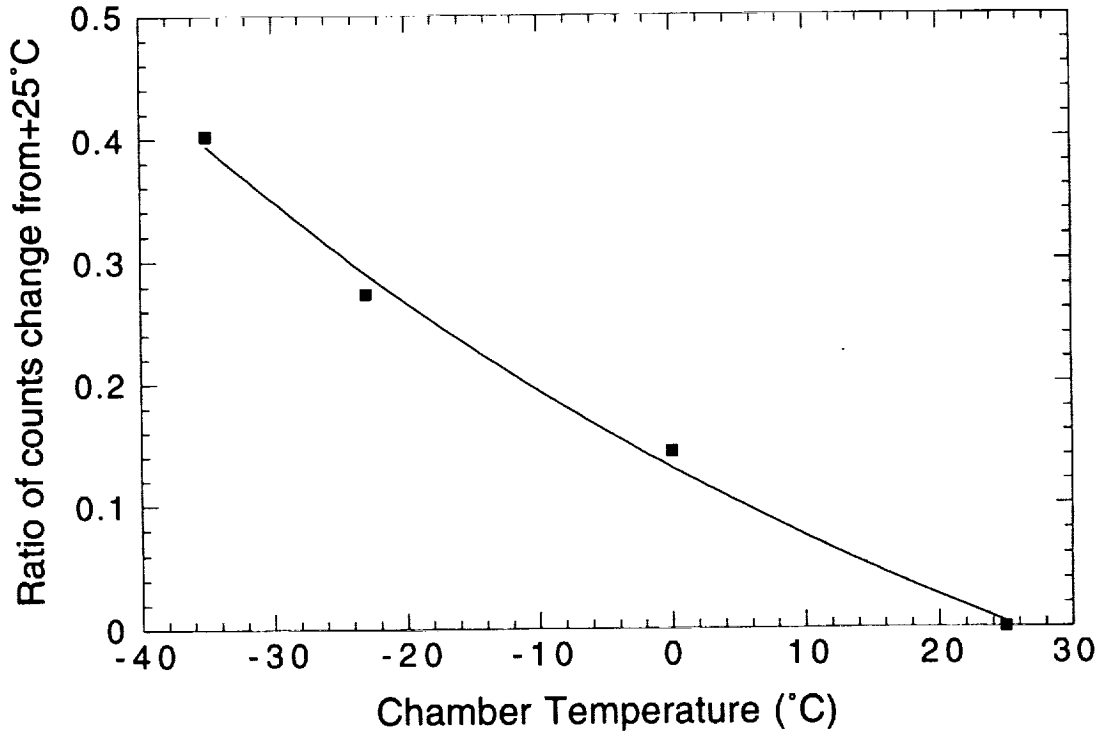


Figure 8. Ratio of the change from laboratory conditions (+25°C) of MAS channel 5 counts to decreasing instrument temperature. Solid line is an exponential best fit curve.

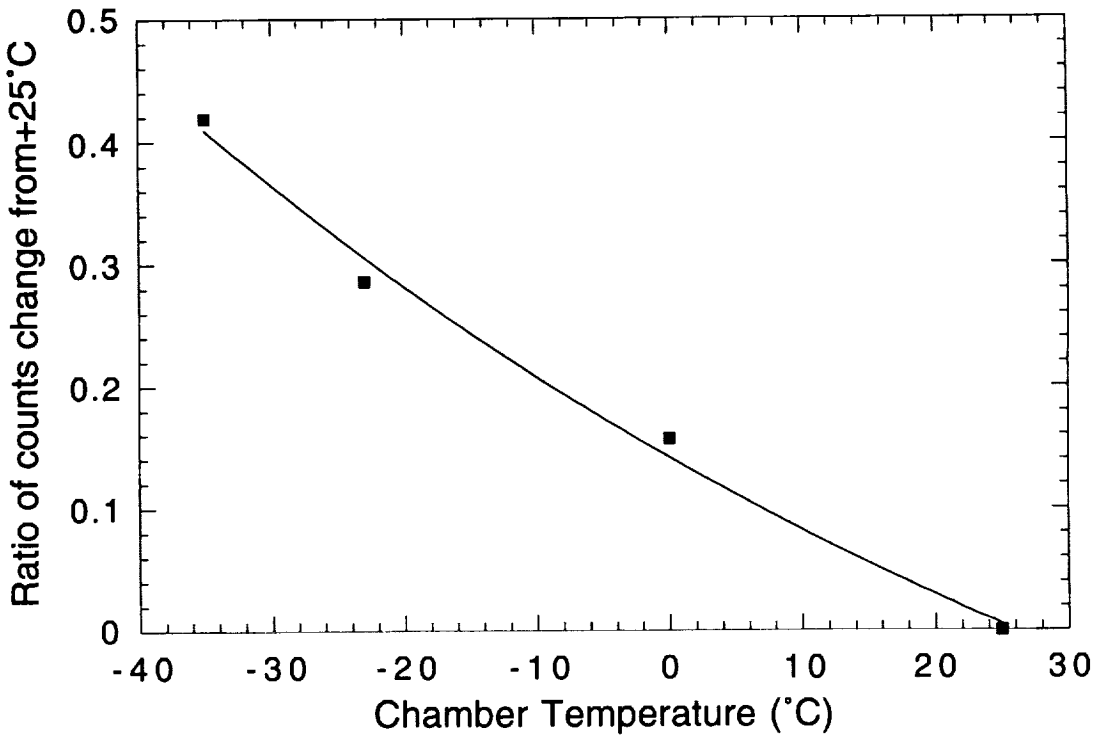


Figure 9 Ratio of the change from laboratory conditions (+25°C) of MAS channel 6 counts to decreasing instrument temperature. Solid line is an exponential best fit curve.

Channel 6:

$$\Delta mas_4 = m_1 + m_2 * \exp(-m_3 * T_{mas}), \quad \text{where,} \tag{5}$$

$m_1$ =-0.41817
$m_2$ = 0.55977
$m_3$ = 0.01118

To convert the in-flight measured counts to the equivalent value at +25°C, the change in the MAS measurement ratio ($\Delta mas_n$) must be applied to the in-flight counts value (after subtracting the offset). This is demonstrated by the following equation:

$$C_{+25} = C_T/(1-\Delta mas_n), \quad \text{where,} \tag{6}$$

$C_{+25}$ - the effective counts value at laboratory conditions (+25°C); before adding offset
$C_T$ - at temperature T, the recorded in-flight counts value minus the appropriate offset
$\Delta mas_n$ - for channel number n, the ratio of the change in MAS counts from +25°C to the value at instrument temperature T divided by the counts at +25°C (with offsets subtracted from all counts values)

Next to get the actual counts value ($C_{lab}$) to which the coefficients in Table 6 can then be directly applied, the offset counts must be added to $C_{+25}$. Thus:

$$C_{lab} = C_{+25} + (C_0 * g). \tag{7}$$

Using equation 7, equation 5 is substituted in for the $C_{+25}$ term, and then equations 1-4 as appropriate for each channel, are substituted for the $\Delta mas_n$ term. This results in set of four equations (one per channel) which can be used to convert any in-flight counts value (at any gain) to the appropriate effective value at 25°C. The four equations are :

Channel 3:

$$C_{lab} = (C_{infl}-(C_0*g)) / (1.02637 - 0.09183 * \exp(-0.03872*T_{mas})) + (C_0*g), \quad \text{where,} \qquad (8)$$

- $C_{lab}$ - the effective counts value at laboratory conditions (+25°C), the counts value to actually apply the calibration coefficients to
- $C_{infl}$ - the recorded in-flight counts value
- $T_{mas}$ - the MAS instrument temperature (°C)
- $C_0$ - offset counts (number of counts recorded when observing cold blackbody) - note MAS data system always records $C_0$ at a gain setting of 1.0. Also it is recommend that a running average of about 30 scans be used to smooth the $C_0$ values
- g - gain setting for $C_{infl}$ (necessary to convert $C_0$ to the same gain as $C_{infl}$)

Channel 4:

$$C_{lab} = (C_{infl}-(C_0*g)) / (1.06322 - 0.13954 * \exp(-0.03148*T_{mas})) + (C_0*g), \qquad (9)$$

Channel 5:

$$C_{lab} = (C_{infl}-(C_0*g)) / (1.31486 - 0.44537 * \exp(-0.01329*T_{mas})) + (C_0*g), \qquad (10)$$

Channel 6:

$$C_{lab} = (C_{infl}-(C_0*g)) / (1.41817 - 0.55977 * \exp(-0.01118*T_{mas})) + (C_0*g). \qquad (11)$$

Note some caution is necessary in the use of the above equations, since in the chamber tests, flight conditions are only partially simulated. Cooling rates of any temperature sensitive parts might be quite different in the chamber as compared to in the aircraft pod. Also in the chamber the pressure is not reduced and therefore no effects due to the low pressure can be simulated. More testing in a thermal vacuum chamber would be helpful to determine more accurately the calibration change at temperature for future deployments.

## V. Intercomparison of Field Calibration to Ames 30-Inch Sphere Calibration

Before and after deployment, the MAS visible and near-infrared channels are calibrated at Ames using a 30-inch integrating sphere. Using this data, for every MAS flight, a calibration summary is produced and distributed to the principle investigator and archived in the flight files. In this summary the radiance/count values at gain of 1 are divided by the actual gain settings used on the specific data flight to yield the appropriate coefficients for that mission. When changes in the instrument occur during deployment affecting system performance, comments documenting these changes accompany the documentation.

To calibrate the MAS, the instrument is placed directly over the sphere either in the Ames lab or while mounted in the plane. No mirror is necessary. With six lamps illuminated in the sphere, data is recorded and digital counts are noted. The mean of the nadir point provides the digital counts that are incorporated with the sphere radiance, lamp intensity, offset value (recorded observation of blackbody #1) and bandpass curves to produce a calibration coefficient of radiance/count at a gain of one. Radiance/count at a gain of 1 is calculated by

equation 12 below.

$$L_{cgl} = (L_i * I_{nl})/((C_s - (C_0 * g_s)) / g_s)), \quad \text{where,} \qquad (12)$$

$L_{cgl}$ = radiance per count @ gain = 1 (slope of counts to radiance conversion)

$L_i$ = in-band sphere radiance with all six lamps illuminated, calculated by integrating the sphere radiance data over the MAS spectral bandpass (sphere radiance for peak response function wavelength in bandpass when full bandpass filter function is unavailable)

$I_{nl}$ = adjustment factor for the number of lamps used during the calibration run (measured empirically by Optronic Labs)

$C_s$ = raw counts viewing sphere

$C_0$ = offset counts or tare value, taken while viewing blackbody #1 The MAS data system always records this value at a gain of 1

$g_s$ = gain setting used while viewing the sphere

The Ames 30-inch sphere, which has been in use since 1987, is calibrated by Optronic Laboratories Inc. on nearly an annual basis. Optronic determines the near normal spectral radiance of the exit aperture over the wavelength range of 350 to 2400 nm. Measurements are made at 10 nm intervals in the visible near-IR region, and at 20 nm interval in the IR. Three measurements are made; one with lamps 1, 2, 5, 6, 9, and 10 operating, one with lamps 3, 4, 7, 8, 11, and 12 operating, and lamp intensity values of one through twelve lamps. During most calibration runs, only six of the twelve lamps in the sphere are utilized at one time because the brightness exceeds most instruments tolerances. There is an average variance between these sets of lamps of only 0.9 percent. Overall, with five measurements since 1988 there has been an average of only 6 % variance between the yearly measurements. The radiance values for the Ames sphere for the FIRE-Cirrus deployment are listed in Table 9.

Also in Table 9 are the peak wavelength values (wavelength of the maximum spectral response) for each MAS visible and near-IR channel and the associated radiance value (term $L_i$ in eqn. 12) computed for the peak wavelength of each MAS channel and (for the 0.681, 1.617, and 2.139 μm channels) the radiance determined by integrating the radiance over the factory measured spectral response curves. The response curves were measured on 11/11/91 and are shown in Figures 10, 11, and 12 as plots of wavelength vs. percent response. The two methods of determining the 'in-band' radiance values in Table 9 show that their differences (for three channels presented here) are small. The radiance values for the two methods are nearly identical for the 0.681 and 1.617 μm channels (<1%) and only about 2% different in for the 2.139 μm channel.

The integrated radiance values for the 0.681, 1.617, and 2.139 μm channels (MAS channels 2, 3, and 6) and the peak wavelength radiance for the 1.933 and 2.088 channels (channels 4 and 5) were then used in equation 12 to calculate the radiance/count factor for each channel. Table 10 summarizes the MAS channels 2-6 calibration results (observing the Ames 30-inch sphere) just prior to the ER-2's departure from Ames to Houston and upon its arrival back at Ames after the FIRE-Cirrus deployment.

Table 9. Radiance Values for the Ames 30-Inch Sphere as Measured on 2/6/91 With Lamps 1, 2, 5, 6, 9, 10 Illuminated, and Corresponding MAS Radiance Calculated Both from the Bandpass Peak Power Point, and Integrated (Weighted) Over the Bandpass Filter.

| Wavelength (μm) | Ames Sphere | MAS Peak Power Wavelength (μm) | Radiance at Peak Power Point W $m^{-2}$ $\mu m^{-1}$ $sr^{-1}$. | Radiance Integrated w/bandpass W $m^{-2}$ $\mu m^{-1}$ $sr^{-1}$. |
|---|---|---|---|---|
| 0.50 | 77.0 | | | |
| 0.55 | 116.0 | | | |
| 0.60 | 157.1 | | | |
| 0.65 | 195.7 | | | |
| 0.70 | 229.3 | 0.681 | 217.846 | 217.461 |
| 0.75 | 251.2 | | | |
| 0.80 | 269.8 | | | |
| 0.85 | 282.2 | | | |
| 0.90 | 287.8 | | | |
| 0.95 | 281.4 | | | |
| 1.00 | 273.1 | | | |
| 1.05 | 263.6 | | | |
| 1.10 | 252.4 | | | |
| 1.15 | 236.4 | | | |
| 1.20 | 219.3 | | | |
| 1.25 | 207.2 | | | |
| 1.30 | 195.2 | | | |
| 1.35 | 170.3 | | | |
| 1.40 | 147.0 | | | |
| 1.45 | 122.6 | | | |
| 1.50 | 120.2 | | | |
| 1.55 | 115.7 | | | |
| 1.60 | 107.4 | 1.617 | 105.403 | 106.177 |
| 1.65 | 101.5 | | | |
| 1.70 | 95.2 | | | |
| 1.75 | 82.8 | | | |
| 1.80 | 72.1 | | | |
| 1.85 | 64.2 | | | |
| 1.90 | 45.6 | 1.933 | 38.084 | |
| 1.95 | 37.6 | | | |
| 2.00 | 42.0 | | | |
| 2.05 | 40.5 | 2.088 | 36.270 | |
| 2.10 | 35.0 | | | |
| 2.15 | 36.1 | 2.139 | 37.377 | 36.652 |
| 2.20 | 30.8 | | | |

Table 10. Ames Pre and Post FIRE-Cirrus Radiance/Count Values and Their Ratio

| Channel | Wavelength | Ames pre-FIRE | Ames post-FIRE | Ratio post/pre |
|---|---|---|---|---|
| 2 | 0.681 | 0.0919 | 0.1525 | 1.659 |
| 3 | 1.617 | 0.0335 | 0.0348 | 1.039 |
| 4 | 1.933 | 0.0150 | 0.0150 | 1.000 |
| 5 | 2.088 | 0.0314 | 0.0311 | 0.990 |
| 6 | 2.139 | 0.0363 | 0.0356 | 0.981 |

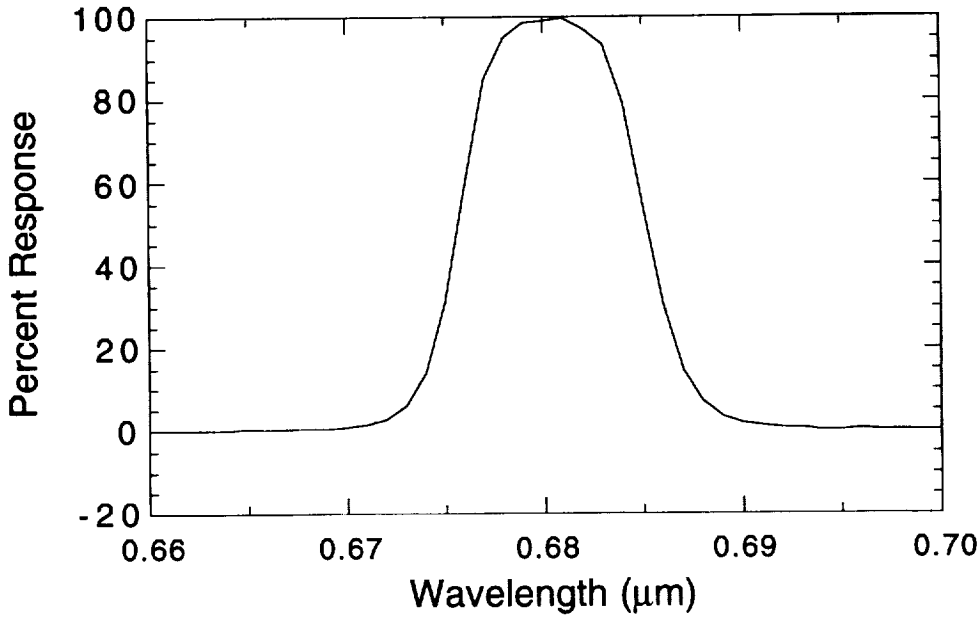


Figure 10. MAS channel 2 spectral bandpass filter. Peak power point is at 0.681 μm.

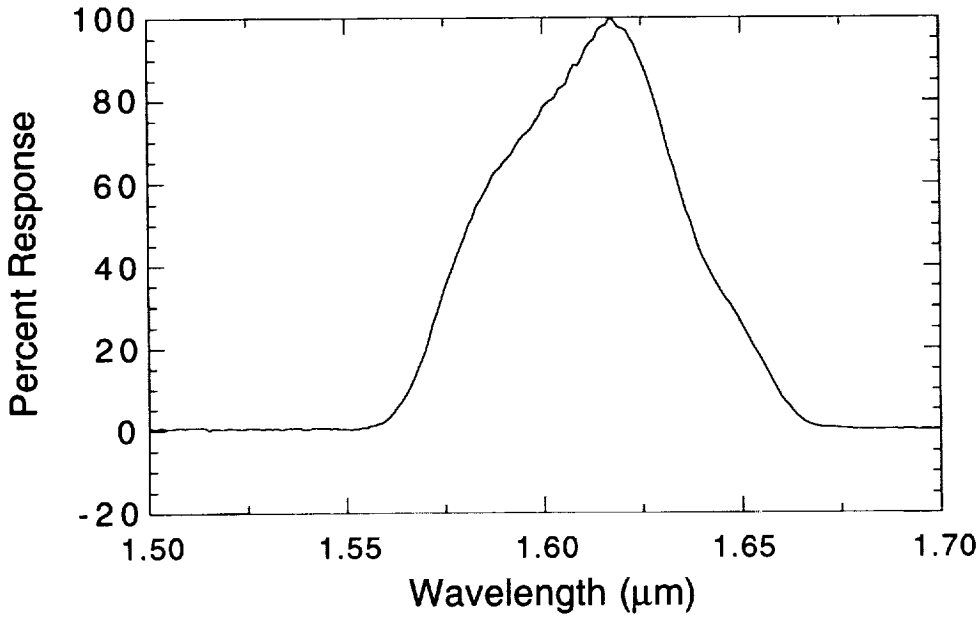


Figure 11. MAS channel 3 spectral bandpass filter. Peak power point is at 1.617 μm.

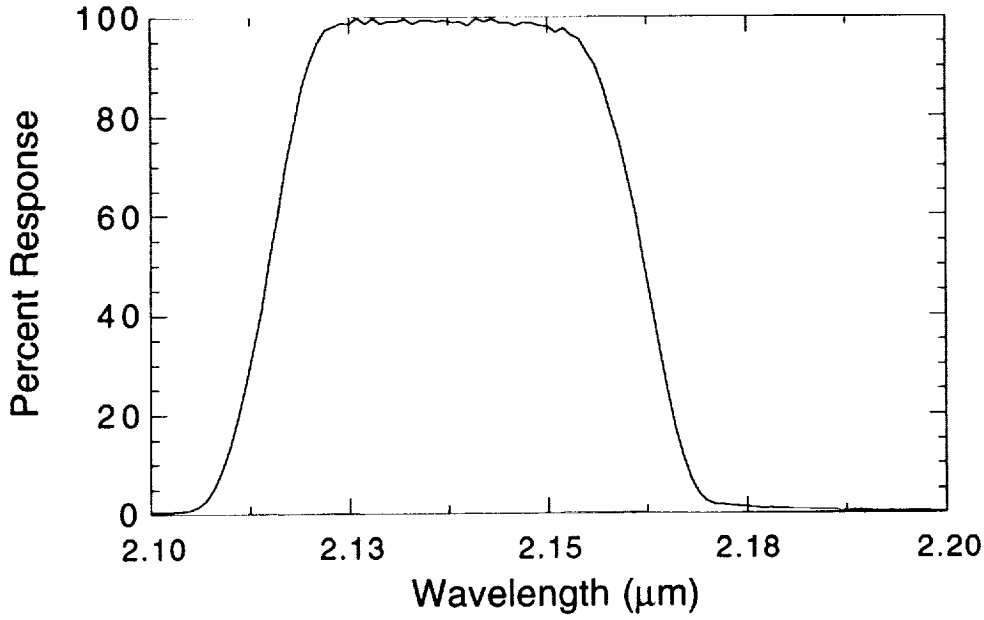


Figure 12. MAS channel 6 spectral bandpass filter. Peak power point is at 2.139 μm.

Generally the agreement between the two calibrations is quite good. The substantial difference in channel 2 is largely due to a resistor change made on 15 November during the deployment. The resistor change was necessary due to a saturation condition in the MAS electronics that 'clipped' the counts at a value less than the maximum possible value of 255 counts. According to the type of the resistors installed, the radiance/count value for channel 2 for the Ames pre-FIRE-Cirrus data should increase by about 100%. This would increase the radiance/count value of 0.0919 in Table 10 to value of 0.1836. Compared to the Ames post-FIRE-Cirrus data this value is somewhat larger. However inspection of the raw counts for the Ames pre-FIRE-Cirrus calibration data suggests that the 'clipping' affected the calibration. The averaged raw counts value for channel 2, at a gain setting of 0.5 observed at the 6 lamp setting of the sphere was 121 counts. Analysis of the flight data on 14 November (92-027) shows clipping at 122 counts. This suggests that the sphere calibration could well have been affected by the clipping (the one count difference could easily be explained by instrument noise and/or some smaller data values being averaged into the sphere data). Thus it is likely the sphere raw counts value that would have been recorded had there been no clipping would have been some unknown amount higher. Increasing the counts values above the recorded value would have the effect of decreasing the radiance/count (from the 1.836 value) and likely improving the agreement. As a result of the apparent clipping problem, the radiance/count value in Table 10 for pre-FIRE-Cirrus channel 2 is considered suspect.

To compare the Goddard hemisphere calibration values (from Table 6), to the Ames results, an average was taken of the pre and post-FIRE Ames data (channel 2 pre-FIRE-Cirrus radiance/count value was not used). The resulting average calibration values for the Ames data are compared to the 48-inch hemisphere values (from Table 6) in Table 11 below. The agreement for channel 2 is quite good. However for the other four channels the agreement is quite poor. Why this agreement is so poor is not proven. The hemi/Ames ratio is consistently higher for channels 3-6 (all near-IR channels), suggesting some type of a systematic difference. One possible explanation are the detectors use to calibrate the light sources in the near-IR region . If either the Goddard or Optronic near-IR detectors were in error, this would explain why channel 2 (which uses a different detector) was not affected. Long trend tracking of AMES and Goddard calibration sources however suggests that the detec-

tors/sources are not likely the problem. A second possible explanation, the use of the 45° inclined mirror for the hemisphere calibration, also does not likely explain the difference, since channel 2 should have been more strongly affected that 3-6. (Mirror radiance adjustment is adjust about 16% for channel 2 but only about 2-4% for the other channels.) A third explanation, use by Ames personnel of the spectral response curves in the calibration (rather than just using the central wavelength for each channel as in the hemisphere calibration analysis) also does not explain the difference since this difference has already been demonstrated to be small and also response curves were not used for channels 4 and 5. The most likely answer is that the Ames MAS calibration measurements for FIRE were taken too soon after the port 2 dewar was filled. As discussed previously in section III, it is necessary to allow time for the signal in the near-IR channels to stabilize due to the cooling from the LN2 vapors produced while filling the MAS dewars. As a result the attenuated data in the AMES test should be thrown out. Further analysis from intercomparisons with satellite and AVIRIS data would be useful in providing additional supporting evidence of the calibration difference.

Table 11. Comparison of the Hemisphere Radiance/Count Values for FIRE-Cirrus Data With the Average of Ames Pre and Post FIRE-Cirrus Radiance/Count Values

| Channel | Wavelength (μm) | AMES Avg | Hemisphere | Hemi/Ames |
|---|---|---|---|---|
| 2 | 0.681 | 1.525 | 1.498 | 0.982 |
| 3 | 1.617 | 0.342 | 0.4114 | 1.203 |
| 4 | 1.933 | 0.150 | 0.1938 | 1.292 |
| 5 | 2.088 | 0.313 | 0.3879 | 1.239 |
| 6 | 2.139 | 0.360 | 0.4242 | 1.178 |

Note channel 2 pre-FIRE-Cirrus radiance/count value was not used to calculate the channel 2 Ames avg. value.

## VI. Future Calibration Work

All future light source calibrations (beginning in 1994) will be conducted every 0.01 μm. Also rather than using just the radiance at the peak spectral response (as in section III), the source radiance value for each MAS channel will routinely be determined by integration over the appopriate spectral bandpass of each MAS channel. In addition future publications will describe in much greater detail possible error sources in the calibration, and also a report will be issued on the results of labratory tests (conducted at Ames) of spectral noise (shifting) for each MAS channel.

# REPORT DOCUMENTATION PAGE

*Form Approved*
*OMB No. 0704-0188*



| 1. AGENCY USE ONLY *(Leave blank)* | 2. REPORT DATE | 3. REPORT TYPE AND DATES COVERED |
|---|---|---|
| | March 1994 | Technical Memorandum |

**4. TITLE AND SUBTITLE**
MODIS Airborne Simulator Visible and Near-Infrared Calibration - 1991 FIRE-Cirrus Field Experiment
*Calibration Version - FIRE King 1.1*

**5. FUNDING NUMBERS**
913

**6. AUTHOR(S)**
G. Thomas Arnold, Michael Fitzgerald, Patrick S. Grant, and Michael D. King

**7. PERFORMING ORGANIZATION NAME(S) AND ADDRESS (ES)**
Goddard Space Flight Center
Greenbelt, Maryland 20771

**8. PEFORMING ORGANIZATION REPORT NUMBER**
94B00054

**9. SPONSORING / MONITORING ADGENCY NAME(S) AND ADDRESS (ES)**
National Aeronautics and Space Administration
Washington, DC 20546-0001

**10. SPONSORING / MONITORING ADGENCY REPORT NUMBER**
NASA TM-104600

**11. SUPPLEMENTARY NOTES**
Arnold: Applied Research Corporation, Landover, Maryland; Fitzgerald and Grant: ATAC, Mountain View, California; King: Goddard Space Flight Center, Greenbelt, Maryland

**12a. DISTRIBUTION / AVAILABILITY STATMENT**
Unclassified - Unlimited
Subject Category 47

**12b. DISTRIBUTION CODE**

**13. ABSTRACT** *(Maximum 200 words)*
Calibration of the visible and near-infrared channels of the MODIS Airborne Simulator (MAS) is derived from observations of a calibrated light source. For the 1991 FIRE-Cirrus field experiment, the calibrated light source was the NASA Goddard 48-inch integrating hemisphere. Laboratory tests during the FIRE-Cirrus field experiment were conducted to calibrate the hemisphere and from the hemisphere to the MAS. The purpose of this report is to summarize the FIRE-Cirrus hemisphere calibration, and then describe how the MAS was calibrated from observations of the hemisphere data. All MAS calibration measurements are presented, and determination of the MAS calibration coefficients (raw counts to radiance conversion) is discussed. Thermal sensitivity of the MAS visible and near-infrared calibration is also discussed. Typically, the MAS in-flight is 30 to 60 degrees C colder than the room temperature laboratory calibration. Results from in-flight temperature measurements and tests of the MAS in a cold chamber are given, and from these, equations are derived to adjust the MAS in-flight data to what the value would be at laboratory conditions. ForFIRE-Cirrus data, only channels 3 through 6 were found to be temperature sensitive. The final section of this report describes comparisons to an independent MAS (room temperature) calibration by Ames personnel using their 30-inch integrating sphere.

**14. SUBJECT TERMS**
Calibration - radiometric, remote sensing - instrumentation, MODIS, MODIS Airborne Simulator, ASTEX, FIRE-cirrus

**15. NUMBER OF PAGES**
32

**16. PRICE CODE**

| 17. SECURITY CLASSIFICATION OF REPORT | 18. SECURITY CLASSIFICATION OF THIS PAGE | 19. SECURITY CLASSIFICATION OF ABSTRACT | 20. LIMITATION OF ABSTRACT |
|---|---|---|---|
| Unclassified | Unclassified | Unclassified | UL |